ACS Medicinal Chemistry Letters

pubs.acs.org/acsmedchemlett

Vorinostat-Like Molecules as Structural, Stereochemical, and Pharmacological Tools

Stephen Hanessian,*[,†] Luciana Auzzas,[†,‡] Andreas Larsson,[†,§] Jianbin Zhang,[†] Giuseppe Giannini,*[,∥] Grazia Gallo,[∥] Andrea Ciacci,[∥] and Walter Cabri[∥]

[†]Department of Chemistry, Université de Montréal, P.O. Box 6128, Station Centre-ville, Montréal, QC, H3C 3J7, Canada, [‡]Istituto di Chimica Biomolecolare, Consiglio Nazionale delle Ricerche, Traversa La Crucca 3, I-07040 Sassari, Italy, [§]Department of Chemistry, Umeå University, 901 87, Umeå, Sweden, and [∥]Sigma-Tau Research & Development, Via Pontina Km 30.400, I-00040 Pomezia, Roma, Italy

ABSTRACT The inhibitory activity of an ω-alkoxy analogue of the HDAC inhibitor, Vorinostat (SAHA), against the 11 isoforms of HDAC is described and evaluated with regard to structural biology information retrieved through computational methods. Preliminary absorption and metabolism studies were performed, which positioned this compound as a potential candidate for further preclinical studies and delineated measures for improving its pharmacokinetic profile.

KEYWORDS HDAC promiscuous inhibitors, SAHA analogues, HDAC1−11 profile, class IIa-specific profile, absorption and metabolism

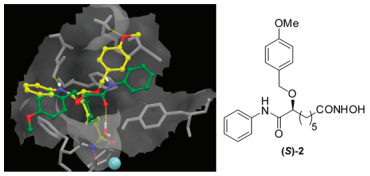

In spite of the significant progress made in HDAC research,[1−4] the quest for isoform-selective inhibitors continues to present a major challenge.[5−7] To date, detailed biostructural information is available only regarding a few among the known 11 metallo-enzymes.[1,8−11] Consequently, the design of isoform- and class-selective inhibitors is somewhat arbitrary and derivative.[1,7,12−14] In addition, complete data regarding the factual HDAC profile for most of the early discovered agents are not available, since the development of effective isozyme-based assays is relatively recent.[5−7,15−18] As a consequence of the complex, pleiotropic nature of cancer, promiscuous HDAC inhibitors such as Vorinostat (**1**) (SAHA, suberoylanilide hydroxamic acid)[19] (Figure 1) seem superior and as safe in the clinic as compared to the few class-specific agents available.[5−7,15]

Ligand-based approaches are a first-choice solution to delineate the structural requirements for HDAC selectivity, especially with the emergence of ω-aryl alkanoyl hydroxamates such as Vorinostat as clinical candidates.[1,7,12−14] In this regard, simple and readily accessible surrogates are worthy of study, provided that they bear pharmacophoric determinants as close as possible to a maximum common substructural consensus required to target the whole HDAC panel. The judicious inclusion of specific appendages capable of interacting with specific residues in the cap region of HDACs can provide valuable structural, functional, and stereochemical insight into the design of new inhibitors.

In a previous study, we determined the optimal alkyl chain length for activity against a single isoform, HDAC2.[20] Designed for understanding the role of the chirality in simple ω-alkoxy analogues of Vorinostat, compound (*R*/*S*)-**2** emerged as a promising lead for its preliminary cytotoxic activity against leukemia, colon, and lung tumor cell lines. Here, we describe the details for the improved and shortened synthesis of **2**, together with the biostructural insights through molecular modeling and a preliminary study of its in vitro activity against an *extended* panel of HDACs.

Although relatively simple in conception, the previous nine-step synthesis of racemic **2**[20] was shortened and adapted to produce gram-scale material for pharmacological studies (Supporting Information) (Scheme 1). The required 8-carbon chain of (*R*/*S*)-**2** was assembled by a cross metathesis reaction[21] between an excess of methyl acrylate and the olefin **3**, readily available from (*R*/*S*)-glycidol,[22] in the presence of Grubbs' second generation catalyst in CH_2Cl_2 at 40 °C. Catalytic reduction to the methyl ester **4**, followed by $Sc(OTf)_3$-assisted *O*-alkylation with PMB trichloroacetimidate,[23] led to **5**. This was deprotected with TBAF, and the product was submitted to a Swern oxidation to obtain aldehyde **6** in 94% yield for two steps. Jones oxidation of **6** led to the carboxylic acid intermediate, which was immediately coupled as a crude with aniline in the presence of Goodman's reagent (DEBPT),[24] leading to anilide **7** in 75% yield. Finally, conversion to hydroxamic acid (*R*/*S*)-**2** was easily achieved by treating methyl ester **7** with hydroxylamine and NaOH in MeOH. Enantiopure **2** could be obtained starting from (*R*)- or (*S*)-**3** or by Mitsunobu inversion of configuration of the individual alcohols.[20] Using this protocol, the synthesis of (*R*/*S*)-**2** was achieved in seven steps from **3** in 37% overall yield.

In preliminary testing against HeLa immunopurified HDAC2 assay,[20] (*R*/*S*)-**2** exhibited comparable if not improved

Received Date: December 30, 2009
Accepted Date: March 3, 2010
Published on Web Date: March 11, 2010

DOI: 10.1021/ml100028g | *ACS Med. Chem. Lett.* **2010**, *1*, 70–74

nanomolar potency over Vorinostat. Surprisingly, no significant difference in inhibitory activity was found between (*R*/*S*)-**2** and its individual enantiomers against this HDAC isoform.[25] A subsequent antiproliferative evaluation against three different human cancer cell lines (NB4, H460, and HCT-116) substantiated the potential of **2** as a promising candidate for further profiling.

The potency of racemic and enantiopure **2** to inhibit 11 isolated human HDAC isozymes in the presence of a fluorogenic peptide bound to the RHKK(Ac) fragment of p53 (residues 379−382) as the substrate is shown in Table 1.[18] Vorinostat,[19] trichostatin A (TSA),[26] and NVP-LAQ824[27] were used as reference compounds.

From this investigation, we confirmed the role of **2** as a promiscuous inhibitor, displaying an activity comparable to Vorinostat against all HDACs. No significant difference was found between the racemic **2** and its individual enantiomers, which proved to be equipotent against all of the zinc-dependent HDACs. To gain more insight into this equivalence, a docking analysis of the individual enantiomers of **2** was performed based on the crystal structures of HDAC8[8] and HDAC7,[9] which were chosen as representatives of class I and II HDACs, respectively (Figure 2).[28] In binding these isoforms, a T-shape arrangement was observed for both enantiomers of ligand **2**, which projected its aromatic motifs out from the active site channel toward lipophilic pockets located in opposite directions on the enzyme surface. The Phe208 and Phe152 residues in the rim of HDAC8 were found to engage in $\pi-\pi$ interactions with either the anilide or the *p*-methoxybenzyl moieties of each enantiomer. The relative distances between each Phe residue and the aromatic moieties of both enantiomers, together with the corresponding number of interactions, are shown in Table 2.[29] The sum of $\pi-\pi$ interactions produced by the (*S*)- and (*R*)-enantiomers of **2** with both Phe residues was found to be almost the same in HDCA8. Overall, 13 interactions were detected in the case of (*S*)-**2**, and 11 were detected in the case of (*R*)-**2**, which may account for the slight difference shown by the enantiomers in binding this isoform [$IC_{50(R)/(S)}$ = 3.3]. The binding was further stabilized by interactions between the amide bonds of the (*R*)- and (*S*)-isomers with a conserved water molecule as well as with a conserved Asp residue[8] (Asp101 in HDAC8). In addition, a H-bond between the methoxy group of the (*S*)-isomer and the Lys33 in HDAC8 contributed to stabilization of the complex. This Lys residue is peculiar to HDAC8[8] and may also play a part in the small difference in activity between the enantiomers.

Upon binding to HDAC7, analogous interactions were observed in the rim of this isozyme, involving Phe738 (Phe208 in HDAC8), Phe679 (Phe152 in HDAC8), and the aromatic groups of both enantiomers of **2**. In this case, three and four $\pi-\pi$ interactions stabilizing the complex of (*S*)- and (*R*)-**2**, respectively, via their anilide and PMB rings, were recorded as compared to HDAC8 (Table 2). A conserved water molecule stabilized the isomers through interactions with the amide and the ether bonds of (*S*)-**2** and (*R*)-**2**, respectively. An interaction was found between the Asp626 and the amide bond of (*R*)-**2**, which might explain its marginally higher activity over the (*S*)-enantiomer [$IC_{50(S)/(R)}$ = 3.4]. In addition, further $\pi-\pi$ interactions were observed between the Phe737 and the PMB ring of (*R*)-**2** and

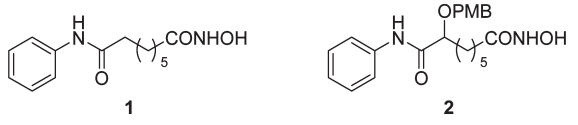

Figure 1. Structure of Vorinostat (SAHA) and the ω-alkoxy analogue **2**.

Scheme 1. Synthesis of ω-Alkoxy Analogue **2**[a]

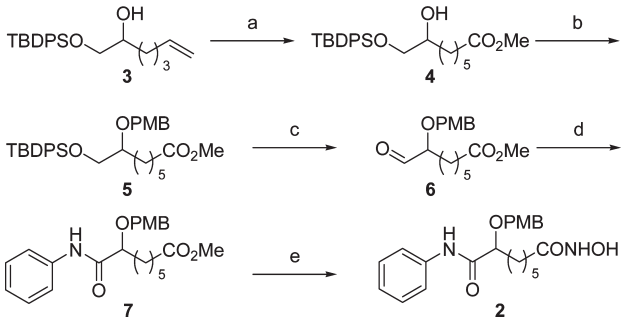

[a] Reagents and conditions: (a) (i) CH_2=$CHCO_2Me$, Grubbs' second generation catalyst (3 mol %), CH_2Cl_2, 40 °C, 1 h (97%); (ii) H_2, Pd−C, MeOH, 18 h (97%). (b) CCl_3C(=NH)OPMB, $Sc(OTf)_3$ (10 mol %), MePh, 0 °C to room temperature, 12 h (58%). (c) (i) TBAF, THF, 0 °C to room temperature, 4 h (95%); (ii) $(COCl)_2$, DMSO, CH_2Cl_2, −78 °C, then Et_3N, −78 °C to room temperature (99%). (d) (i) Jones reagent, 0 °C, 5 min (99%); (ii) DEBPT, DIPEA, THF, then $PhNH_2$, 0 °C to room temperature, 48 h (75%). (e) $HONH_2$(aq), 1.0 N NaOH, MeOH, 0 °C to room temperature (95%).

Table 1. In Vitro Inhibitory Activity of Racemic and Enantiopure **2** against HDAC1−11 Isoforms (IC_{50}, nM)[a]

	HDAC1	HDAC2	HDAC3	HDAC4	HDAC5	HDAC6	HDAC7	HDAC8	HDAC9	HDAC10	HDAC11
Vorinostat	258.00	921.00	350.00	493.00	378.00	28.60	344.00	243.00	316.00	456.00	362.00
TSA	7.12	22.95	10.32	12.07	16.48	0.42	22.46	89.53	38.12	20.10	15.15
NVP-LAQ824	3.23	15.70	10.50	5.82	5.58	5.93	6.11	3.84	8.24	8.41	5.58
(*R*/*S*)-**2**	53.40	254.00	131.00	648.00	134.00	20.10	432.00	331.00	247.00	179.00	197.00
(*S*)-**2**	95.30	234.00	131.00	555.00	205.00	21.00	733.00	236.00	382.00	323.00	278.00
(*R*)-**2**	48.50	122.00	172.50	364.00	151.00	18.10	219.00	781.00	262.00	161.00	189.00

[a] Values are the means of a minimum of three experiments and are given in the nanomolar range. Compound **2** was tested in 10-dose IC_{50} mode in triplicate with 3-fold serial dilution starting from 50 μM solutions. In the case of TSA and Vorinostat, a 10 μM solution was used. Screening was performed by Reaction Biology Corp. (Malvern, PA).

DOI: 10.1021/ml100028g | *ACS Med. Chem. Lett.* 2010, *1*, 70–74

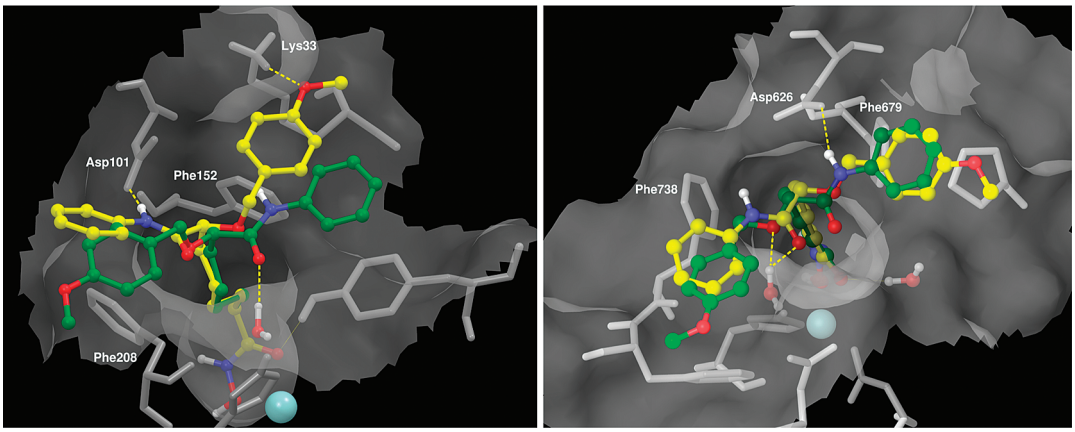

Figure 2. Left: best docking solutions of (*S*)-**2** (yellow) and (*R*)-**2** (green) on HDAC8 crystal structure.[28] Right: best docking solutions of (*S*)-**2** (yellow) and (*R*)-**2** (green) on HDAC7 crystal structure.[28] H-bonds between the ligands and the enzyme are shown as dashed lines. Calculated with Glide v. 5.0 Schrödinger, L.L.C. (New York, www.schrodinger.com). For additional details, see the Supporting Information.

Table 2. $\pi-\pi$ Interaction Distances (Å) and Number of Interactions[29] between the Aromatic Rings of (*S*)- and (*R*)-**2** and the Phe Residues in the Rim of HDAC8 (Phe208 and Phe152) and HDAC7 (Phe738 and Phe679)[a]

	HDAC8			HDAC7			
	Phe208	no. of interactions (Phe208)	Phe152	no. of interactions (Phe152)	Phe738	no. of interactions (Phe738)	Phe679	no. of interactions (Phe679)
(*S*)-**2**	3.5−4.9 (Anil)	6	4.9−5.6 (PMB)	7	4.3 (Anil)	1	5.2−5.5 (PMB)	3
(*R*)-**2**	3.7−4.4 (PMB)	7	4.1−5.0 (Anil)	4	5.0 (PMB)	1	4.9−5.3 (Anil)	3

[a] Anil, anilide ring; PMB, *p*-methoxybenzyl ring.

the anilide motif of (*S*)-**2**, equally reinforcing the binding of both enantiomers.

Despite the different Phe binding interaction sites observed for the two isomers of **2** against these HDACs, the levels of their inhibitory activity were not appreciably changed. Overall, their binding mode suggested that the lipophilic interactions had a major role in stabilizing their individual complexes.[30] In part, our hypothesis is also confirmed by a detailed structural comparison between HDAC1 and HDAC8.[31] Considering the high level of conservation of Phe residues among the HDAC isoforms,[8−11] these interactions might explain the lack of discrimination between the individual enantiomers.

It has been recently argued that the enzymatic activity associated with class IIa HDACs ectopically expressed in mammalian cells might be the result of a residual contamination by class I HDACs present in class IIa immunocomplexes.[16] In view of this possibility, we deemed it necessary to extend our assay to include this method of HDAC profiling with (*R*/*S*)-**2**. The in vitro test was performed in the presence of the class IIa-specific fluorogenic substrate acetyl-Lys-(trifluoroacetyl)-AMC, using Vorinostat and TSA as the reference compounds (Table 3; see also the Supporting Information). Given the low sensitivity of this substrate, a remarkable decrease in the activity for all of the tested compounds was observed, which was in the micromolar range. For this reason, the two enantiomers of **2** were not tested. Although compound (*R*/*S*)-**2** was found to be as active as Vorinostat against HDAC7 and HDAC9, and slightly less active against HDAC5, *it was totally inactive toward HDAC4*.

Table 3. In Vitro Inhibitory Activity of (*R*/*S*)-**2** against Class IIa HDAC Isoforms (IC_{50}, μM)[a]

	HDAC4	HDAC5	HDAC7	HDAC9
Vorinostat[b]	6.64	5.51	49.5	56.3
TSA	7.92	2.56	4.23	5.59
(*R*/*S*)-**2**	>1000	24.8	82.8	58.6

[a] Values are the means of a minimum of three experiments and are given in the micromolar range. Substrate concentration, 10 μM. [b] Data from Reaction Biology Corp. (http://www.reactionbiology.com/HDACS/HDACsClass2ASub%20Controlcurves.pdf).

Thus, a dramatic difference was observed between the activities of (*R*/*S*)-**2** and Vorinostat in the class IIa-specific assay against HDAC4, as compared to the results shown in Table 1 in the class I-II-IV profiling assay. As suggested by the Gallinari group,[16] this might be due to the presence of a residual deacetylase activity from contaminant class I HDACs in traditional profiling assays. The generality of this observation must be validated by a careful scrutiny of the appropriate substrates and the purity of recombinant isoenzymes enabling accurate HDAC profiling.[3,5−7,15−17]

Preliminary assays were performed on (*R*/*S*)-**2** to assess its absorption and metabolism. Human colorectal carcinoma-derived cells (Caco-2 cell line) were used as an established in vitro model for the prediction of (*R*/*S*)-**2** absorption across the human intestine.[32] A transport study was performed to obtain apparent permeability coefficients (P_{app}) in the apical to basolateral direction, and the result was compared to

DOI: 10.1021/ml100028g | *ACS Med. Chem. Lett.* **2010**, *1*, 70–74

Vorinostat and to the reference compounds cimetidine, vinblastine, and caffeine (Supporting Information). According to this model, a high intestinal permeability can be predicted for P_{app} coefficients higher than 50. In this assay, a good level of oral absorption was predicted for (*R*/*S*)-**2**, which showed a P_{app} value higher than Vorinostat (P_{app} = 219.2 vs P_{app} = 77.6 nm/s) and comparable to caffeine (P_{app} = 312.4 nm/s).

The metabolism study was performed upon incubation of (*R*/*S*)-**2** with human cryopreserved hepatocytes (HC2 and H655) and by subsequent quantification of the remaining parent compound from the incubated supernatant by UPLC.[33] The metabolic stability was defined as the percentage of parent compound lost over time in the active test system. Vorinostat was used as a reference compound, together with 7-ethoxycoumarin and 7-hydroxycoumarin as the positive controls of hepatocyte competence for phase I and II metabolism, respectively (0.42% left after 90 min at 1 μM concentration and 2.08% left under the same conditions).[33] Although a lower stability was observed for (*R*/*S*)-**2** as compared to Vorinostat (23% left after 90 min at 1 μM concentration vs 61% left under the same conditions for Vorinostat), measures for improving its pharmacokinetic profile can be taken based on the chemical modification at specific sites.[34]

In conclusion, we have studied the structural and stereochemical effects of an optimized ω-alkoxy analogue of Vorinostat as a probe to assess its in vitro activity profile against 11 isoforms of HDAC. Although a higher permeability was noted for compound **2** in the Caco-2 assay as compared to Vorinostat, a faster rate of metabolism was observed. It is possible that *O*-demethylation or benzylic carbon oxidation is taking place, which could be avoided with appropriate functional group modifications. Results pertaining to these and other variations will be disclosed in due course.

SUPPORTING INFORMATION AVAILABLE Synthetic procedures, ^{1}H and ^{13}C NMR spectra of hydroxamic acid **2**, experimental procedures for biological assays, molecular modeling procedures, and selection of recent references for complete and partial HDAC profiling. This material is available free of charge via the Internet at http://pubs.acs.org.

AUTHOR INFORMATION

Corresponding Author: *To whom correspondence should be addressed. Tel: +1-514-343-6738. Fax: +1-514-343-5728. E-mail: stephen.hanessian@umontreal.ca. Tel: +39-06-9139-3640. Fax: +39-06-9139-3638. E-mail: giuseppe.giannini@sigma-tau.it.

Funding Sources: We thank NSERC of Canada for financial assistance. A postdoctoral grant from Wenner-Gren Foundation, Sweden, is kindly acknowledged by A.L.

ACKNOWLEDGMENT We thank Dr. Alexandra Furtos, Dalbir Sekong, and Dr. Sylvie Bilodeau of Centre Régional de Spectroscopie and of Service de RMN de l'Université de Montréal for their kind assistance. L.A. thanks the Italian National Research Council (CNR), Institute of Biomolecular Chemistry, Italy, for a sabbatical leave.

REFERENCES

(1) Zhang, L.; Fang, H.; Xu, W. Strategies in Developing Promising Histone Deacetylase Inhibitors. *Med. Res. Rev.* **2009**, DOI: 10.1002/med.20169.
(2) Paris, M.; Porcelloni, M.; Binaschi, M.; Fattori, D. Histone Deacetylase Inhibitors: From Bench to Clinic. *J. Med. Chem.* **2008,** *51*, 1505–1529.
(3) Bolden, J. E.; Peart, M. J.; Johnstone, R. W. Anticancer Activities of Histone Deacetylase Inhibitors. *Nat. Rev. Drug Discovery* **2006,** *5*, 769–784.
(4) Minucci, S.; Pelicci, P. G. Histone Deacetylase Inhibitors and the Promise of Epigenetic (and More) Treatments for Cancer. *Nat. Rev. Cancer* **2006,** *6*, 38–51.
(5) Witt, O.; Deubzer, H. E.; Milde, T.; Oehme, I. HDAC Family: What Are the Cancer Relevant Targets?. *Cancer Lett.* **2009,** *277*, 8–21.
(6) Khan, N.; Jeffers, M.; Kumar, S.; Hackett, C.; Boldog, F.; Khramtsov, N.; Qian, X.; Mills, E.; Berghs, S. C.; Carey, N.; Finn, P. W.; Collins, L. S.; Tumber, A.; Rithchie, J. W.; Jensen, P. B.; Lichenstein, H. S.; Sehested, M. Determination of the Class and Isoform Selectivity of Small-Molecule Histone Deacetylase Inhibitors. *Biochem. J.* **2008,** *409*, 581–589.
(7) Bieliauskas, A. V.; Pflum, M. K. H. Isoform-Selective Histone Deacetylase Inhibitors. *Chem. Soc. Rev.* **2008,** *37*, 1402–1413.
(8) Vannini, A.; Volpari, C.; Gallinari, P.; Jones, P.; Mattu, M.; Carfí, A.; De Francesco, R.; Steinkühler, C.; Di Marco, S. Substrate Binding to Histone Deacetylase as Shown by the Crystal Structure of the HDAC8-Substrate Complex. *EMBO Rep.* **2007**, *8*, 879−884 and references therein.
(9) Schuetz, A.; Min, J.; Allali-Hassani, A.; Schapira, M.; Shuen, M.; Loppnau, P.; Mazitschek, R.; Kwiatkowski, N. P.; Lewis, T. A.; Maglathin, R. L.; McLean, T. H.; Bochkarev, A.; Plotnikov, A. N.; Vedadi, M.; Arrowsmith, C. H. J. Human HDAC7 Harbors a Class IIa Histone Deacetylase-Specific Zinc Binding Motif and Cryptic Deacetylase Activity. *J. Biol. Chem.* **2008,** *283*, 11355–11363.
(10) Bottomley, M. J.; Lo Surdo, P.; Di Giovine, P.; Cirillo, A.; Scarpelli, R.; Ferrigno, F.; Jones, P.; Neddermann, P.; De Francesco, R.; Steinkühler, C.; Gallinari, P.; Carf, A. Structural and Functional Analysis of the Human HDAC4 Catalytic Domain Reveals a Regulatory Structural Zinc-binding Domain. *J. Biol. Chem.* **2008**, *283*, 26694−26704 and references therein.
(11) http://www.actrec.gov.in/histone/infobase.htm.
(12) Hu, F.; Chou, C. J.; Gottesfeld, J. M. Design and Synthesis of Novel Hybrid Benzamide-Peptide Histone Deacetylase Inhibitors. *Bioorg. Med. Chem. Lett.* **2009,** *19*, 3928–3931.
(13) Olsen, C. A.; Ghadiri, M. R. Discovery of Potent and Selective Histone Deacetylase Inhibitors via Focused Combinatorial Libraries of Cyclic $\alpha_3\beta$-Tetrapeptides. *J. Med. Chem.* **2009**, *52*, 7836−7846 and references therein.
(14) Bowers, A. A.; Greshock, T. J.; West, N.; Estiu, G.; Schreiber, S. L.; Wiest, O.; Williams, R. M.; Bradner, J. E. Synthesis and Conformation-Activity Relationships of the Peptide Isosteres of FK228 and Largazole. *J. Am. Chem. Soc.* **2009,** *131*, 2900–2905.
(15) Blackwell, L.; Norris, J.; Suto, C. M.; Janzen, W. P. The Use of Diversity Profiling to Characterize Chemical Modulators of the Histone Deacetylases. *Life Sci.* **2008,** *82*, 1050–1058.
(16) Lahm, A.; Paolini, M.; Pallaoro, M.; Nardi, M. C.; Jones, P.; Nedderman, P.; Sambucini, S.; Bottomley, M. J.; Lo Surdo, P.; Carfí, A.; Koch, U.; De Francesco, R.; Steinkühler, C.; Gallinari, P. Unraveling the Hidden Catalytic Activity of Vertebrate Class IIa Histone Deacetylases. *Proc. Natl. Acad. Sci. U.S.A.* **2007,** *104*, 17335–17340.

(17) Bradner, J. E.; West, N.; Grachan, M. L.; Greenberg, E. F.; Haggarty, S. J.; Warnow, T.; Mazitschek, R. Chemical Phylogenetics of Histone Deacetylases. *Nat. Chem. Biol.* **2010**, *6*, 238−243 and references therein.

(18) For a recent example of HDAC profiling in the development of a potent inhibitor, see the following: Arts, J.; King, P.; Mariën, A.; Floren, W.; Beliën, A.; Janssen, L.; Pilatte, I.; Roux, B.; Decrane, L.; Gilissen, R.; Hickson, I.; Vreys, V.; Cox, E.; Bol, K.; Talloen, W.; Goris, I.; Andries, L.; Du Jardin, M.; Janicot, M.; Page, M.; van Emelen, K.; Angibaud, P. JNJ-26481585, a Novel `Second Generation' Oral Histone Deacetylase Inhibitor, Shows Broad-Spectrum Preclinical Antitumoral Activity. *Clin. Cancer Res.* **2009,** *15*, 6841–6851. For further selected examples, see the Supporting Information.

(19) Marks, P. A.; Breslow, R. Dimethyl Sulfoxide to Vorinostat: Development of This Histone Deacetylase Inhibitor as an Anticancer Drug. *Nat. Biotechnol.* **2007,** *25*, 84–90.

(20) Hanessian, S.; Auzzas, L.; Giannini, G.; Marzi, M.; Cabri, W.; Barbarino, M.; Vesci, L.; Pisano, C. ω-Alkoxy Analogues of SAHA (Vorinostat) as Inhibitors of HDAC: A Study of Chain-Length and Stereochemical Dependence. *Bioorg. Med. Chem. Lett.* **2007,** *17*, 6261–6265.

(21) Chatterjee, A. K.; Choi, T.-L.; Sanders, D. P.; Grubbs, R. H. A General Model for Selectivity in Olefin Cross Metathesis. *J. Am. Chem. Soc.* **2003,** *125*, 11360–11370.

(22) Dixon, D. J.; Ley, S. V.; Tate, E. W. A Total Synthesis of (+)-Goniodiol Using an Anomeric Oxygen-to-Carbon Rearrangement. *J. Chem. Soc., Perkin Trans. 1* **1998,** 3125–3126.

(23) Rai, A. N.; Basu, A. An Efficient Method for para-Methoxybenzyl Ether Formation with Lanthanum Triflate. *Tetrahedron Lett.* **2003,** *44*, 2267–2269.

(24) Li, H.; Jiang, X.; Ye, Y.-H.; Fan, C.; Romoff, T.; Goodman, M. 3-(Diethoxyphosphoryloxy)-1,2,3- benzotriazin-4(3H)-one (DEPBT): A New Coupling Reagent with Remarkable Resistance to Racemization. *Org. Lett.* **1999,** *1*, 91–93.

(25) (*S*) isomers of simple ω-substitute amide derivatives of SAHA have been reported as potent HDAC inhibitors, although any relationship about chirality was not described; see the following: Richon, V.; Marks, P. A.; Rifkind, R. A.; Breslow, R.; Belvedere, S.; Gershell, L.; Miller, T. A. Novel Class of Cytodifferentiating Agents and Histone Deacetylase Inhibitors, and Methods of Use Thereof. WO0118171-A2, 2001.

(26) Mori, K.; Koseki, K. Synthesis of Trichostatin A, a Potent Differentiation Inducer of Friend Leukemic Cells, and Its Antipode. *Tetrahedron* **1988,** *44*, 6013–6020.

(27) Remiszewski, S. W. The Discovery of NVP-LAQ824: From Concept to Clinic. *Curr. Med. Chem.* **2003,** *10*, 2393–2402.

(28) High-resolution HDAC8/MS-344 and HDAC7/TSA complexes were used (PDB codes: 1T67 and 3C10, respectively). These are better resolved than the cocrystals of SAHA with the same HDACs (1T69 and 3COZ, respectively). In addition, a water molecule is present only in 1T67, which is thought to be responsible for the stabilization of MS-344 through its amide bond. See ref 8.

(29) Calculated with LPC software. This is freely accessible at http://bip.weizmann.ac.il/oca-bin/lpccsu. Sobolev, V.; Sorokine, A.; Prilusky, J.; Abola, E. E.; Edelman, M. Automated Analysis of Interatomic Contacts in Proteins. *Bioinformatics* **1999**, *15*, 327−332.

(30) Davis, A. M.; Teague, S. J. Hydrogen Bonding, Hydrophobic Interactions, and Failure of the Rigid Receptor Hypothesis. *Angew. Chem., Int. Ed.* **1999,** *38*, 736–749.

(31) Ortore, G.; Di Colo, F.; Martinelli, A. Docking of Hydroxamic Acids into HDAC1 and HDAC8: A Rationalization of Activity Trends and Selectivities. *J. Chem. Inf. Model.* **2009,** *49*, 2774–2785.

(32) Gres, M.-C.; Julian, B.; Bourrié, M.; Meunier, V.; Roques, C.; Berger, M.; Boulenc, X.; Berger, Y.; Fabre, G. Correlation Between Oral Drug Absorption in Humans, and Apparent Drug Permeability in TC-7 Cells, a Human Epithelial Intestinal Cell Line: Comparison with the Parental Caco-2 Cell Line. *Pharm. Res.* **1998,** *15*, 726–733.

(33) Li, P. E.; Lu, C.; Brent, J. A.; Pham, C.; Fackett, A.; Ruegg, C. E.; Silber, P. M. Cryopreserved Human Hepatocytes: Characterization of Drug-Metabolizing Enzyme Activities and Applications in Higher Throughput Screening Assays for Hepatotoxicity, Metabolic Sability, and Drug-Dug Interaction Potential. *Chem.-Biol. Interact.* **1999,** *121*, 17–35.

(34) For a comparison of pharmacokinetics of Vorinostat with certain mercaptoacetamides, see the following: Konsoula, R.; Jung, M. *Int. J. Pharm.* **2008**, *361*, 19−25.

DOI: 10.1021/ml100028g | *ACS Med. Chem. Lett.* **2010**, *1*, 70–74